Reprinted from INTERNATIONAL JOURNAL OF THERMOPHYSICS

Vol. 7, No. 2, March 1986
Printed in Belgium

Isochoric Specific Heat of Sulfur Hexafluoride at the Critical Point: Laboratory Results and Outline of a Spacelab Experiment for the D1-Mission in 1985[1]

J. Straub,[2] R. Lange,[3] K. Nitsche,[2] and K. Kemmerle[4]

The specific heat at constant volume c_v shows a weak singularity at the critical point. Renormalization group techniques have been applied, predicting a universal critical behavior which has to be experimentally confirmed for different systems. In this paper an experiment is presented to measure the specific heat of SF_6 along the critical isochore ($\rho_c = 0.737\ g \cdot cm^{-3}$), applying a continuous heating method. The results cover a temperature span of $-1.5 \times 10^{-2} < \tau < 1.70 \times 10^{-2}$ [$\tau = (T - T_c)/T_c$] and were strongly affected by gravity effects that emerge in the sample of 1-mm hydrostatic height near the critical point. Using regression analysis, data were fitted with functions of the form $c_v/R = A \times |\tau|^{-\alpha} + B$ for the one-phase state and $c_v/R = A'' \times |\tau|^{-\alpha''} + B''$ for the two-phase state. Within their error bounds the critical values ($\alpha = \alpha'' = 0.098$, $A''/A = 1.83$) represent the measurements for the temperature span $3.5 \times 10^{-5} < |\tau| < 2.0 \times 10^{-3}$, in good agreement with theoretical predictions. In order to exclude density profiles in the specimen, which are unavoidable in terrestrial experiments due to the high compressibility of fluids at the critical point and the gravity force, a space-qualified scanning ratio calorimeter has been constructed, which will permit long-term c_v measurements under microgravity (μ-g) conditions. The experiment will be part of the German Spacelab mission in October 1985. The significant features of the apparatus are briefly sketched.

KEY WORDS: critical phenomena; critical exponents; isochoric specific heat; scanning ratio calorimeter; microgravity.

[1] Paper presented at the Ninth Symposium on Thermophysical Properties, June 24–27, 1985, Boulder, Colorado, U.S.A.

[2] Lehrstuhl A fur Thermodynamik, Technische Universität München, Arcisstr. 21, D-8000 München 2, Federal Republic of Germany.

[3] Schubert und Salzer, Fr.-Ebert-Str. 84, D-8070 Ingolstadt, Federal Republic of Germany.

[4] Kayser-Threde GmbH, Wolfratshauserstr. 44, D-8000 München 70, Federal Republic of Germany.

0195-928X/86/0300-0343$05.00/0

1. INTRODUCTION

As one of its basic tasks, experimental thermodynamics includes measuring material properties of real fluids, for example, with respect to technical equations of state that are based almost exclusively on empirical data. For some special thermodynamic states, however, for example, the critical point of a pure fluid, macroscopic properties such as the specific heat at constant volume c_v can be theoretically derived. Especially, renormalization group techniques have been applied, which yield numerical values for critical exponents [1] and amplitude ratios [2, 3] which are to be experimentally verified.

The experimental access of the critical point, in particular of the specific heat c_v, is beset by special difficulties due to the increased sensibility of the fluid sample to external fields. In order to measure the weak critical c_v anomaly, a high-resolution scanning ratio calorimeter has been developed. With the continuous-heating technique applied, small temperature ramps $dT/dt = 1\ \mu\mathrm{K} \cdot \mathrm{s}^{-1}$ were realized that guaranteed thermodynamic equilibrium close to the critical temperature despite the enhanced relaxation times. In addition, gravity generates density sedimentations and leads to "somehow" averaged results not being representative for a thermodynamic *point* of state. In terrestrial (1-g) experiments this effect is partly compensated by reducing the hydrostatic height of the specimen cell (here 1 mm) but canot be excluded completely [4].

The German Spacelab mission D1 in October 1985 will open an opportunity to perform long-term c_v measurements under microgravity (μ-g) conditions. In the preparation of this program two objectives were pursued: First, the efficiency of the measuring concept had to be proved with respect to special conditions in Spacelab (a brief outline of the space-qualified apparatus is given in this paper). Second, c_v was measured along the critical isochore in a temperature span of $|T - T_c| < 5$ K. The results will serve as the 1-g reference for the μ-g data obtained from orbit.

2. EXPERIMENTAL APPARATUS

The mechanical setup of the scanning ratio calorimeter used is shown in Fig. 1. It resembles the one developed by Buckingham et al. [5] for c_v measurements of CO_2 and the one used by Würz and Grubic [6] for c_p measurement of binary liquid mixtures.

The mechanical structure consists of four cylindrical vessels (Stages 0–3) boxed inside each other. The aluminum vacuum cylinder (Stage 3), kept at a constant temperature by means of a water thermostat, generates a thermally stable environment and is evacuated (10^{-5} mbar) to minimize

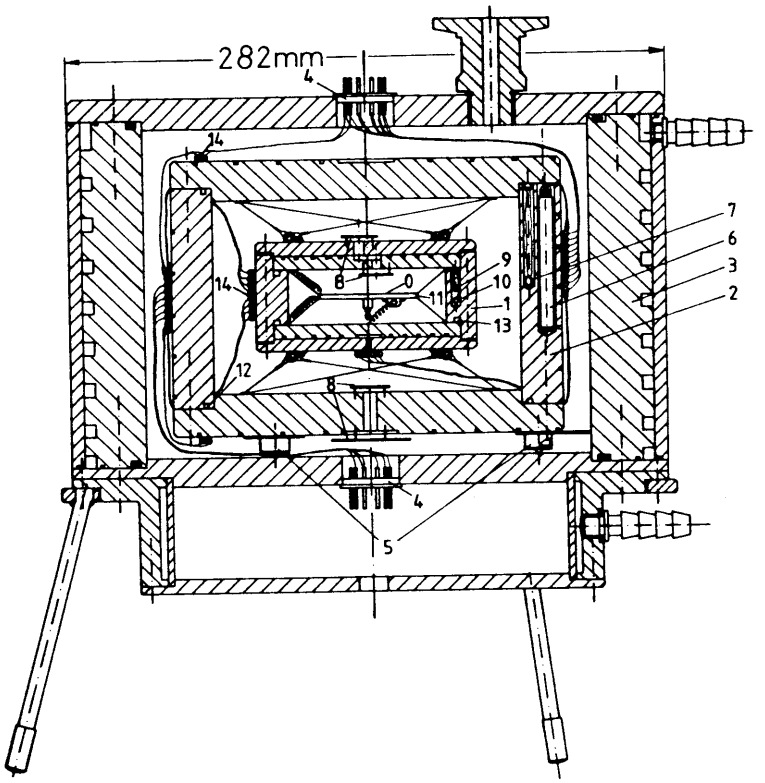

Fig. 1. Mechanical setup of the four-stage scanning ratio calorimeter. 0, Specimen cell; 1, reference stage; 2, adiabatic shield; 3, vacuum cylinder; 4, bushing; 5, insulation supports; 6, Pt 25; 7, thermistor; 8, emissivity shield; 9/10, thermistor; 11, cell heater; 12, circumferencial; 13, grooves; 14, connectors.

heat leaks between the cylinders. The adiabatic shield (Stage 2), consisting of nickel-plated copper, houses a platinum resistance thermometer (Rosemount 162 D) for measuring the overall process temperature and rests on three plasic supports. Reference Stage 1, also nickel-plated copper, and the sample cell (Stage 0) are suspended on eight thin (12-μm-diameter), separate polyamid threads (Kevlar) with little thermal conductivity ($\lambda = 0.05\ \mathrm{W \cdot m^{-1} \cdot K^{-1}}$). To reduce radiation heat transfer by emissivity, stages 0 and 1 and the inside of Stage 2 are polished. For the electrical circuits enameled copper wires (0.05 mm in diameter) are used, which are coiled to extend the thermal paths of the parasitic heat losses. Before the wires bridge the gaps they are looped in a circumferential groove and thus thermally contacted to the stages.

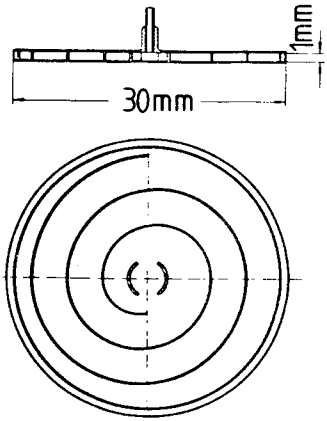

Fig. 2. Specimen cell.

The structure of the coin-shaped test cell (Stage 0) (Fig. 2) is similar to that of the one designed in Ref. 5. It meets three requirements: (i) a low heat capacity of the stainless-steel container (at $T = T_c$, $C_{cont}/C_{fluid} \approx 1/1.2$), (ii) sufficient mechanical resistance ($p = 38$ bar), and (iii) a small hydrostatic height for terrestrial (1-g) measurements.

Inside the cell a machined spiral supports the transverse faces soldered together. As a result, thermal diffusion lengths are minimized and thermal equilibrium is eased. An interior height of less than 1 mm is not very suitable on Earth, owing to the explicit gravitational influences [4] that then would gain dominance. Leakage through microcontraction cavities in the walls of 0.2-mm thickness was avoided by using vacuum-refined material. The critical density of the specimen (SF_6 of 99.993% liquid purity, Matheson Gas Products) was determined by a weighing procedure in comparison with a known reference volume. Taking the thermal and pressure expansion of the cell into account, the overall error of $\pm 0.5\%$ was calculated to be less than the error of the critical density $\rho_c = 0.737\ \mathrm{g \cdot cm^{-3}}$ found in the literature (e.g., Ref. 7 and private communication with Michels, from the van der Waals Laboratory). Several cycles of evacuating (24 h) and flushing the cell guaranteed a high specimen purity.

The functional diagram of the system is shown in Fig. 3. A constant current source supplies Stage 1 with adjustable power, linearly raising the temperature T_1. Control loops 0 and 1 balance the temperatures between the stages such that $T_0 - T_1$ and $T_2 - T_1$ are less than 10 μK, the resolution limit. Each loop consists of an AC bridge equipped with thermistors (Yellow Springs Instruments Type 44031), a lock-in amplifier (L), and an

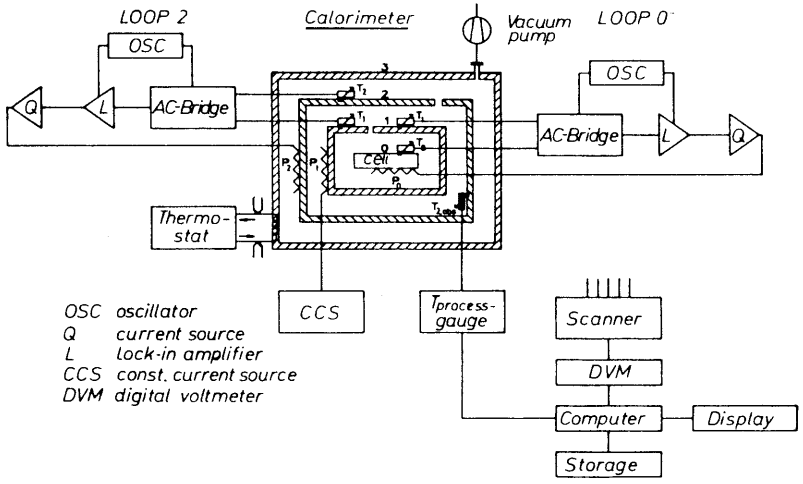

Fig. 3. Functional chart of the calorimeter.

analogly controlled current source (Q). Designs for similar differential thermometers were proposed in Refs. 8–10. Sensitivities of $V_B = dU/dT = 0.9\ \text{mV} \cdot \text{K}^{-1}$ were achieved with a thermistor dissipation of 0.22 μW. By artificial aging, the drift rate of the thermistors, expressed as a fictitious temperature change, was reduced to $2\ \mu\text{K} \cdot \text{h}^{-1}$, which is in good agreement with Refs. 11 and 12.

Of essential importance is the conformity of the characteristic "resistance–temperature" (RT) of both thermistors in one loop. A constant shift can be compensated by bridge adjusting. However, different gradients dR/dT cause the bridge signal to be dependent not only on the temperature differences, but on the process temperature itself. This effect can be minimized by preselecting a pair of thermistors with similar temperature coefficients and was also considered in the final data evaluation.

After an initial adjustment of the AC bridges and the amplifiers, the complete experiment runs for several days without requiring further activities. Thirty-four measurement values per scan were automatically recorded via a scanner, a digital voltmeter, and a digital temperature gauge by means of a HP-1000 computer. High data rates and full automation qualified the experiment to be included in the German μ-g Spacelab program.

3. MEASUREMENT METHOD

An energy balance applied on stages 0 and 1 yields a system of diffential equations,

$$C_0(dT_0/dt) = P_0 + P_{T,0} + \dot{Q}_{01} \tag{1}$$

$$C_1(dT_1/dt) = P_1 + P_{T,1} + \dot{Q}_{01} + \dot{Q}_{12} \tag{2}$$

where $C_0(dT_0/dt)$ denotes the capacity of Stage 0 times the temperature ramp, P_0 the electical heating power, $\dot{Q}_{01}$ the heat leakage from 0 to 1, and $P_{T,0}$ the electrical power dissipated in the thermistor. For P_i measurements a four-wire technique is applied. $\dot{Q}_{ij} = k_{ij}(T_i - T_j)$ is calculated from the measured temperature difference $T_i - T_j$ and the transfer coefficient k_{ij} determined by the relaxation behavior of an unbalanced stage toward thermal equilibrium. Equations (1) and (2) are coupled by the corrected AC-bridge output signal

$$U_B = V_B(T_1 - T_0) + C_B\left(\frac{T_1 + T_0}{2} - T_{BL}\right) \tag{3}$$

with the bridge amplification $V_B = dU/dT$ and C_B correcting the diverging thermistor characteristics in the vicinity of T_{BL}, the temperature at which the AC bridge is balanced. Deriving Eq. (3) with respect to time t combines the energy balance (1 and 2) to an explicit function for the capacity $C_0(T)$, oscillations due to the lock-in amplification being neglected. $C_0(T)$ is further decomposed into

$$C_0(T) = C_{0,\text{container}} + m_{\text{fluid}} \cdot c_{v,\text{fluid}}(T) \tag{4}$$

where $c_{v,\text{fluid}}(T)$ is the specific heat of the test fluid to be measured versus temperature. Capacity

$$C_1(T) = (P_1 + P_{T,1})/(dT_1/dt) \tag{5}$$

of reference Stage 1 was determined for large gradients $(dT_1/dt) = 100\ \mu\text{K} \cdot \text{s}^{-1}$) such that parasitic heat flows $\dot{Q}_{ij}$ could be neglected. The relative temperature coefficient of $6.7 \times 10^{-4}\ \text{K}^{-1}$ agrees well with common values for copper.

4. RESULTS

Curves of the specific heat c_v for different temperature ramps are plotted in Fig. 4. Near the critical state, the data clearly exhibit a systematic deviation which becomes more distinct as dT/dt increases.

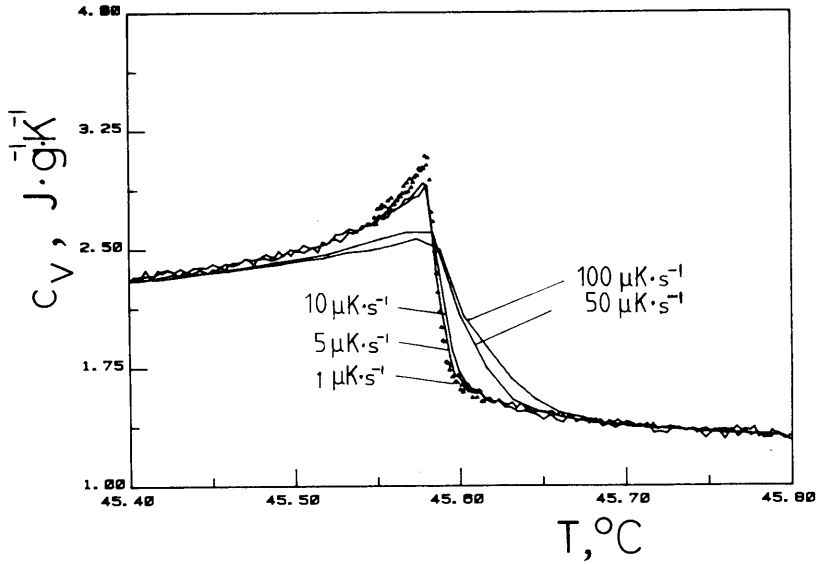

Fig. 4. Measured values of the specific heat c_v for different temperature ramps dT/dt.

These differently sharp peaks from the non-steady-state measurement technique and the delay of establishing thermodynamic equilibrium. The question is, How close to the critical temperature can equilibrium be expected for a given dT/dt?

A quantity for that is the time constant T_{rel}, which characterizes an unbalanced system relaxing to its thermodynamic equilibrium. T_{rel} shows a considerable increase in the critical state [13–15]. Although the physical mechanisms are not completely known, an estimation was made considering only the transient temperature relaxation inside the cell.

Continuous heating generates a finite temperature difference ΔT in the fluid, falsifying a measured value.

$$c_v(T) = c_{v,0} + (\partial c_v/\partial T)_0 \cdot \Delta T \tag{6}$$

The requirement that the measured value matches the equilibrium value $c_{v,0}$ (i.e., $c_v/c_{v,0} \approx 1$) yields

$$|(1/c_{v,0})(\partial c_{v,0}/\partial T)_0 \, \Delta T| < 1 \tag{7}$$

Using the definitions of the thermal time constant

$$\Delta T = T_{rel}(dT/dt) = H^2(dT/dt)/(\pi^2 a) \tag{8}$$

with H being the characteristic length [Eq. (7)], together with the scaling functions for thermal diffusivity

$$a = a_0 |\tau|^{\psi} \tag{9}$$

and for specific heat [Eq. (12)], a quantitative estimation can be deduced:

$$\frac{H^2(dT/dt)}{\pi^2 \quad T_c} \frac{\alpha A |\tau|^{-(1+\alpha+\psi)}}{a_0[A|\tau|^{-\alpha} + B]} = \varepsilon(\tau) \ll 1 \tag{10}$$

with values substituted for diffusivity [16, 17] and specific heat (this paper), equilibrium is to be expected for $|\tau| > 3.5 \times 10^{-5}$, $[(T - T_c) > 0.011\ \mathrm{K}]$, given a 1-mm-high cell and assuming $dT/dt = 1\ \mu\mathrm{K} \cdot \mathrm{s}^{-1}$. With a ramp of $dT/dt = 5\ \mu\mathrm{K} \cdot \mathrm{s}^{-1}$ equilibrium establishes for $|\tau| > 8 \times 10^{-5}$. Inside this temperature span both measurements coincide (Fig. 5). Thus the outlined method permits at least a rough estimation.

On the critical isochore phase transition occurs at critical temperature T_c. The averaging influence of gravity, however, shifts the peak of c_v to subcritical temperatures. Hohenberg and Barmatz [4] estimated this effect for xenon and different hydrostatic heights of the test cell. Here, for a height of 1 mm a shift was computed to $\Delta T_c \approx 3$ mK, leading to a critical

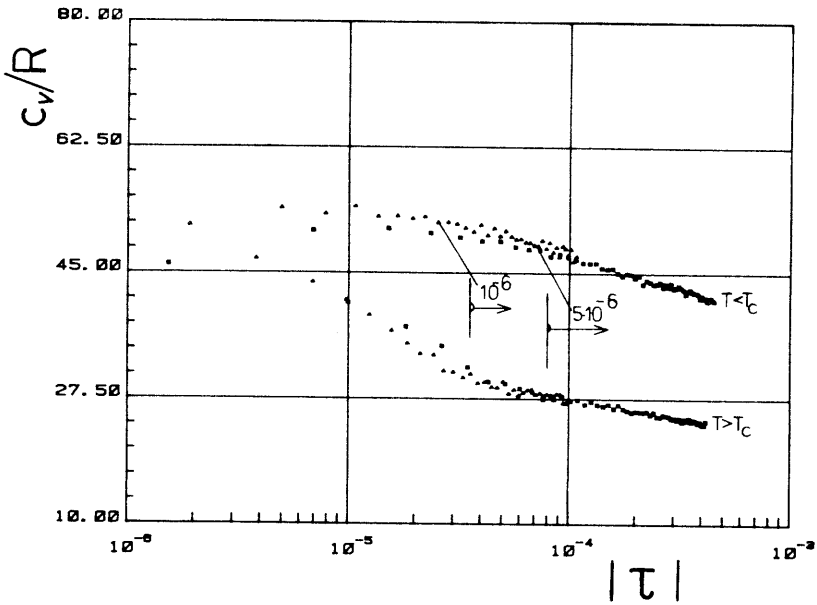

Fig. 5. Thermodynamic equilibrium for different temperature ramps.

temperature $T_c = 45.583°C$, which is in good agreement with Refs. 18–21. An overall error analysis revealed a relative error of $\delta c_v/c_v = 1.5\%$ for $dT/dt = 100\ \mu K \cdot s^{-1}$ and $\delta c_v/c_v = 3.7\%$ for $dT/dt = 1\ \mu K \cdot s^{-1}$.

5. SCALING

For further processing data subsets of different time ramps were joined. The span around the critical temperature was covered with data of the smallest temperature ramp ($1\ \mu K \cdot s^{-1}$) neighbored by sets of the next steeper temperature ramp for sub- and supracritical temperatures, and so on. This procedure was continued until the extracted data file contained 960 points, covering an interval of $-1.5 \times 10^{-2} < \tau < 1.7 \times 10^{-2}$ and showing an increasing data density toward the critical temperature T_c. All points represent equilibrium values except in the immediate vicinity of T_c [Eq. (10)]. For data scaling a least-squares fitting was applied, considering statistical errors of the specific heat *and* of the temperature.

Basically, an extended model of the following form can be chosen:

$$c_v/R = A|\tau|^{-\alpha}[1 + D|\tau|^{x}] + E\tau + B \tag{11}$$

with T_c being an additional free parameter. However, for $x'' = x = 0.5$, as proposed by Barmatz et al. [22], E was obtained to $E = 23.0$ and

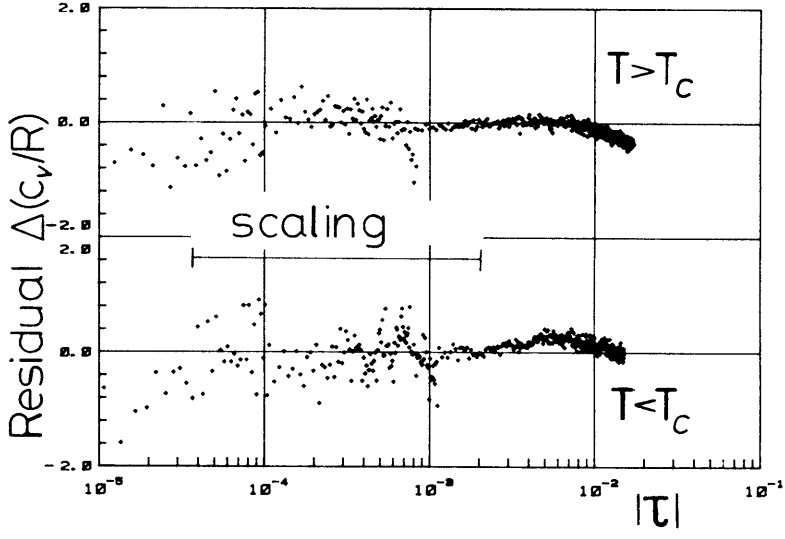

Fig. 6. Residual for the "simple" model [Eq. (12)], i.e., measured value − function value.

$E = -36.5$, which already shows that Eq. (11) could not describe our data. For measurements on a binary system Bloemen et al. [23] over a temperature span twice as wide, the extended model (11) did not yield satisfying results either.

Based upon the "simple" model

$$c_v/R = A|\tau|^{-\alpha} + B \tag{12}$$

a nonlinear regression analysis was carried out, separately for the two- and the one-phase states, with the critical temperature value T_c kept constant for the present. Two bounds limit the interval. The reduced temperature was taken out: (i) $|\tau| = 3.5 \times 10^{-5}$ (condition for equilibrium) and (ii) $|\tau| = |\tau_0|$. In several runs τ_0 was increased until a systematic deviation of the residual

$$(c_v/R)_{\text{measured}} - A|\tau|^{-\alpha} - B \tag{13}$$

emerged. According to Fig. 6, reasonable data fitting is limited for $|\tau_0| = 2 \times 10^{-3}$. However, reducing the interval toward the equilibrium bound ($|\tau_0| \to 3.5 \times 10^{-5}$) led to enhanced uncertainties of the parameter.

Consequently, as Table I reveals, α and B can be set equal within their error spans for both sides of the phase transition. Hence, data were fitted again. Under the constraint $\alpha'' = \alpha$ and $B'' = B$, the fit quickly stabilized. The entire data set and the least-squares fits with an without gravity corrections for $|\tau| < 2 \times 10^{-3}$ are plotted in Fig. 7.

In several additional computations A, α, and B were again determined for different values of the critical temperature T_c. The minimum of the square sum was obtained for $T_c = 45.583°C$.

Table I. Parameter Values for the Simple Model Expressed by Eq. (12), $(\tau) < 2 \times 10^{-3}$

Separate fit		Common fit
$T < T_c$	$T > T_c$	
$A'' = 22.7 \pm 1.7$	$A = 11.6 \pm 1.4$	$A = 10.00 \pm 0.11$
$\alpha'' = 0.086 \pm 0.004$	$\alpha = 0.090 \pm 0.006$	$\alpha = \alpha = 0.0983 \pm 0.0005$
$B'' = -2.5 \pm 2.0$	$B = 0.7 \pm 1.6$	$B = B'' = 2.60 \pm 0.14$
$A/A = 1.95 \pm 0.28$		$A'' = 18.29 \pm 0.14$
		$A''/A = 1.829 \pm 0.022$

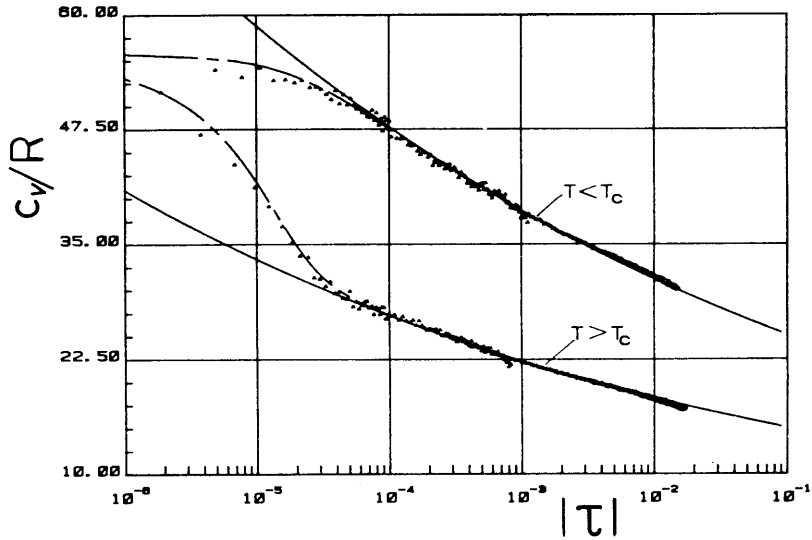

Fig. 7. Specific heat c_v measured values and fit. (△) Measurement; (——) fit; (– – –) fit with gravity correction.

6. COMPARISON WITH THEORY

The Ising model permits a prediction of the critical exponent α and the amplitude ratio A''/A for a fluid at the critical state. The critical results, however, depend slightly on mathematical approximations applied to treat a three-dimensional model. Table II compares the exponent α of this study with theoretical and other experimental investigations. As is further exhibited, the values of α gained from other substances are slightly higher. Despite this, the assumption expressed by Levelt-Sengers et al. [24] cannot be confirmed, that SF_6 might show a systematic deviation from universal behavior. The critical amplitude ratio A''/A, discussed only in more recent publications, is presented in Table III and shows a good agreement with theoretical and experimental values.

Table II. Critical Exponent α, Theoretical and Measured Values

Exponent	Method	Reference
0.125 ± 0.02	Series expansion	Camp et al. [27]
0.110 ± 0.008	Renormalization group technique	Baker et al. [1]
0.098 ± 0.010	c_v measurements of SF_6	This study

Estimate *absolute* error: $\pm 10\%$

Table III. Amplitude Ratios A''/A, Theoretical and Experimental Values

A''/A	Method	References
1.96	Series expansion	Aharony and Hohenberg [27]
1.82	Renormalization group technique	Brézin et al. [3]
2.08	Renormalization group technique	Bervillier [2]
1.86 ± 0.06 ($\alpha = 0.107 \pm 0.005$)	Measured with CO_2	Lipa et al. [11]
1.76 ± 0.03 ($\alpha = 0.107 \pm 0.002$)	Liquid binary mixture	Bloemen et al. [23]
1.83 ± 0.02	Measured with SF_6	This study

7. c_v MEASUREMENTS IN SPACELAB UNDER MICROGRAVITY (μ-g) CONDITIONS

Parallel to laboratory measurements a space-qualified version, "HPT" (high-precision thermostat), of the scanning ratio calorimeter outlined above was developed. The experiment will participate in the German D1 Spacelab mission in October 1985 and permits long-term c_v measurements under μ-g conditions [25]. The mechanical and functional designs correspond in principle to the laboratory version (Figs. 1–3), except for Stage 3 being electrically heated and the heavy Stages 2 and 1, which can be manually locked such that they rest in guiding edges in order to prevent the suspension from being overstrained during shuttle launch. In addition, locking shortens cooling, since heat (except from Stage 0) transfers by conduction across the touching vessel surfaces. The complete apparatus including the power supply, ion-getter pump, and electronic package is housed in a partly thermostabalized 18-in.-high box that fits in a 19-in. rack.

Data relevant for scientific evaluation are encoded in a 12-bit format, housekeeping values in 8-bit words. With a frequency of 128 bytes per 0.6 s data are transferred to an external high-rate multiplexer and, finally, sent to ground in Houston, Texas. With a delay of 0.5 h the experiment is online monitored in the German ground station near Munich. Furthermore, our laboratory computer is linked to the data network and permits quasi-real-time data evaluation, providing a means to advise the astronauts while manually operating the apparatus in case of contingency. The astronauts are trained to handle the HPT equipment and to carry out simple repair work when necessary.

In terrestrial experiments near the critical point relaxation is caused by both reduced thermal diffusivity and density sedimentation, which does not exist in a μ-g environment. To obtain information on the thermal

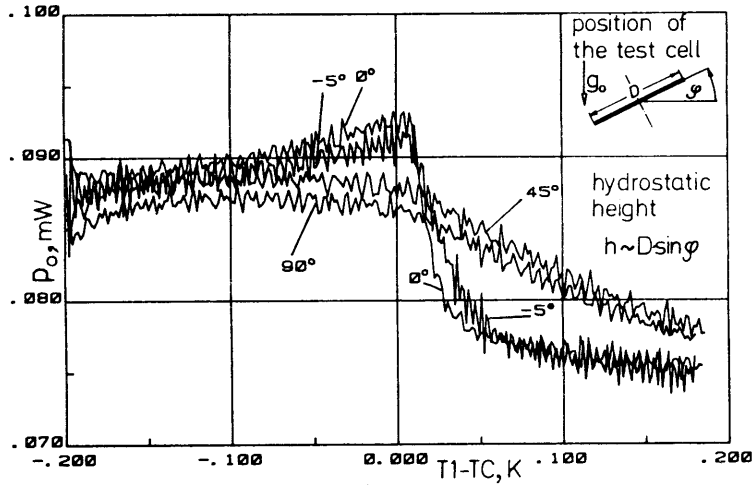

Fig. 8. Heating power P_0 for different hydrostatic heights in the test cell.

relaxation three different temperature gradients are planned that vary in orders of 10: $dT/dt = 3.6$, 10, and 100 mK · h^{-1}. Immediately after the mission, 1-g reference data will be acquired, applying the same time profile.

The μ-g relevance of the HPT experiment is well documented when tilting the calorimeter (Fig. 8). Given a constant power input P in Stage 1, the controlled heating power P_0 of the test cell is proportional to the specific heat [Eq. (1)]. For an inclination angle $\varphi = 0^0$ (the minimum of the hydrostatic height $h = 1$ mm), the characteristic peak at $T_1 - T_c = 0$ reaches its maximum and diminishes as the angle grows to $-5°$ or to $+5°$, respectively. For 45° or, ultimately, at 90° ($h = 30$ mm) the critical enhancement vanishes completely. These data are obtained from a laboratory test of the HPT engineering model.

8. CONCLUSIONS

The continuous measuring technique presented above yields equilibrium values for the specific heat at constant volume c_v of SF_6 close to 0.01 K to the critical point, provided that sufficiently small heating rates ($1\ \mu$ K · s^{-1}) are realized.

The theoretically derived model $c_v/R = A|\tau|^{-\alpha} + B$ [where $\tau = (T - T_c)/T_c$] for the behavior of c_v along the critical isochore is suitable to describe our experimental data measured under terrestrial (1-g) conditions within the temperature intervals $3.5 \times 10^{-5} < (\tau) < 2 \times 10^{-3}$. Data fitting determines the critical exponent to $\alpha = 0.098$ and the amplitude ratio to $A''/A = 1.83$, which is in good agreement with theoretical investigations

and experimental results obtained for different systems. However, the value of α is slightly smaller than postulated by more recent calculations.

Near the fluid critical state density profiles due to gravity falsify c_v measurements and have to be considered in the final data evaluation. Therefore, a calorimeter has been constructed for the German Spacelab mission D1 in 1985 to measure c_v in the immediate vicinity of the critical point under μ-g conditions. Moreover, information is expected about the delayed establishment of the thermodynamic equilibrium in the critical region.

ACKNOWLEDGMENTS

The authors are grateful to the Deutsches Bundesministerium für Forschung und Technologie (BMFT) for financial support of this research. They also wish to express their appreciation to DFVLR for project management.

REFERENCES

1. G. A. Baker, Jr., B. G. Nickel, and P. I. Meiron, *Phys. Rev.* **B17**:1365 (1976).
2. C. Bervillier, *Phys. Rev.* **B14**:4964 (1976).
3. E. Brézin, J. G. Le Guillou, and J. Zinn-Justin, *Phys. Rev.* **D8**:2418 (1973).
4. P. C. Hohenberg and M. Barmatz, *Phys. Rev.* **A6**:289 (1972).
5. M. J. Buckingham, C. Edwards, and J. A. Lipa, *Rev. Sci. Instrum.* **44**:1167 (1973).
6. U. Würz and M. Grubic, *J. Phys. E Sci. Instrum.* **13**:525 (1980).
7. D. Balzarni and P. Palffy, *Can. J. Phys.* **52**:2007 (1974).
8. A. Junod, *J. Phys. E Sci. Instrum.* **12**:945 (1979).
9. N. T. Larsen, *Rev. Sci. Instrum.* **39**:1 (1968).
10. N. Grubic and U. Würz, *J. Phys. E Sci. Instrum.* **11**:693 (1978).
11. J. A. Lipa, C. Edwards, and M. J. Buckingham, *Phys. Rev.* **A15**:778 (1977).
12. S. D. Wood, B. W. Magnum, J. J. Filliben, and S. B. Tillet, *J. Res. NBS* **3**:247 (1978).
13. D. Dahl and M. R. Moldover, *Phys. Rev.* **A6**:1915 (1972).
14. G. R. Brown and H. Meyer, *Phys. Rev.* **A6**:364 (1972).
15. J. Straub, *Proc. 3rd Int. Conf. Chem. Thermodyn.* **2**:40 (1972).
16. H. L. Swinney and H. Z. Cummins, *Phys. Rev.* **171**:152 (1968).
17. E. Reile, P. Jany, and J. Straub, *Wärme- Stoffübertragung* **18**:99 (1984).
18. E. Reile, Dissertation (Technische Universität, München, 1981).
19. W. Rathjen, Dissertation (Technische Universität, München, 1978).
20. H. P. Clegg, J. S. Rowlinson, and J. R. Sutton, *Trans. R. Faraday Soc.* **51**:1327 (1951).
21. A. H. Wentdorff, Jr., *J. Chem. Phys.* **24**:607 (1956).
22. M. Barmatz, P. C. Hohenberg, and A. Kornblit, *Phys. Rev.* **B12**:1947 (1975).
23. E. Bloemen, J. Thoen, and W. Van Dael, *J. Chem. Phys.* **73**:4628 (1980).
24. J. M. H. Levelt-Sengers, W. L. Greer, and J. V. Sengers, *J. Phys. Chem. Ref. Data* **5**:1 (1976).
25. K. Nitsche, R. Lange, and J. Straub, Proceedings of the 5th Symposium on Material Science under μ-g. *ESA SP* **222**:335 (1984).
26. W. J. Camp et al., *Phys. Rev.* **B14**:3990 (1978).
27. A. Aharony and P. C. Hohenberg, *Phys. Rev.* **B13**:3081 (1976).

Printed by the St. Catherine Press Ltd., Tempelhof 41, Bruges, Belgium